Polymer 50 (2009) 1790–1796

Contents lists available at ScienceDirect

Polymer

journal homepage: www.elsevier.com/locate/polymer

Multiple thermosetting of semicrystalline polymers: Polyamide 66 and poly(ethylene terephthalate) fibers

D.R. Salem [a,*], N. Vasanthan [b]

[a] TRI/Princeton, 601 Prospect Avenue, Princeton, NJ 08542, USA
[b] Department of Chemistry, Long Island University, One University Plaza, Brooklyn NY 11201, USA

ARTICLE INFO

Article history:
Received 17 January 2009
Received in revised form
11 February 2009
Accepted 15 February 2009
Available online 24 February 2009

Keywords:
Polyamide 66
Poly(ethylene terephthalate)
Thermosetting

ABSTRACT

Polyamide 66 fibers were thermoset in a torsion-bending deformation at various temperatures up to 240 °C. Some of the fibers were heat-set at constant length prior to the deformation at presetting temperatures of 150 °C and 200 °C to vary the structural state of the starting material. Fractional recovery was measured after various combinations of temperature and time. It was found that heat setting of PA66 is dominated by time-dependent stress relaxation exhibiting time-temperature equivalence. Increased crystallinity, and/or other molecular rearrangements occurring during presetting, impose additional constraints on molecular mobility, which delay onset of the flow regime and increase the time constant of relaxation at a given temperature. The thermosetting characteristics of PA66 fibers are very similar to those of poly(ethylene terephthalate) fibers. For both polymers, superposing the curves of fractional recovery vs. setting time at different temperatures produce satisfactory master curves, without the need for vertical shifting of the data. Arrhenius plots yield approximate activation energies for the thermosetting flow process of 35–65 kcal/mol in PA66 and 95–115 kcal/mol in PET.

1. Introduction

Various industrial processes subject oriented polymers, including polyamide and poly(ethylene terephthalate) fibers, to multiple thermosetting operations. (See, for example, the review by Schultz [1]). Whereas microstructure development during heat-treatment of PA and PET fibers has been increasingly well-characterized [1–18], the capability to predict the thermosetting efficiency resulting from a given thermal sequence has not been established or adequately addressed.

It is well known that stress relaxation in amorphous polymers at temperatures above the glass transition display time–temperature equivalence, and predictive capability is well established [19,20]. For a long time, it was generally inferred that crystalline polymers do not possess this property, and that release of stress sufficient for thermosetting can only be achieved by the melting of small or imperfect crystallites at temperatures well below the final melting point of the polymer [21], which is not a time-dependent process. Data showing extremely slow stress decay in polyethylene at various temperatures supported this view [22]. However, polyethylene usually has a high degree of crystallinity, and it was later shown that polymers of lower crystallinity, such as oriented poly(ethylene terephthalate) [23] and polyamide 66 [24] possess strongly time-dependent stress-relaxation behavior. Moreover, there are some intriguing indications that simple time–temperature superposition may be applicable to these oriented polymers despite their crystallinity and despite the development of additional crystallinity during the stress relaxation process.

The objective of the present paper on polymer thermosetting is to examine detailed information on the temperature–time behavior of polyamide 66 and poly(ethylene terephthalate) fibers that will permit quantitative prediction of setting efficiency under a wide-range of thermal sequences. In addition we will discuss the effects of polymer microstructure on heat setting efficiency.

2. Experimental

2.1. Materials

The experiments were performed with a partially oriented polyamide 66 yarn supplied by DuPont, chosen for its commercial significance. The yarn was 70 denier, with 34 filaments of circular cross-section. It was stored at a relative humidity of 40% and a temperature of 23 °C.

Data collected on polyethylene terephthalate heat-setting in the paper by Buckley and Salem [23] was further analyzed in the

* Corresponding author. Present address: Charge Injection Technologies Inc. Tel.: +1 609 558 8606.
E-mail address: dsalem@chargedinjection.com (D.R. Salem).

0032-3861/$ – see front matter © 2009 Elsevier Ltd. All rights reserved.
doi:10.1016/j.polymer.2009.02.018

present study. The fiber used in that work was a circular PET monofilament, with a draw ratio of 4.

2.2. Presetting

Some of the yarn samples were preset at constant length prior to the heat-setting experiments described below. The presetting time t_p was 30 min and presetting temperatures T_p of 150 °C and 200 °C were used. These presetting temperatures were chosen to provide significant changes in the crystallinity of the fibers, as will be shown later, and to lie in a temperature range of commercial interest.

2.3. Heat-setting in torsion-bending

Heat-setting of the polyamide 66 fibers was carried out according to a procedure similar to that applied in the heat setting studies of the PET monofilament [23]. The experimental steps were as follows: (1) apply strain by twisting the yarn 5 turns and clamping; (2) heat the clamped yarn (at constant length) in a pre-heated air oven at the setting temperature T_s for a time t_s; (3) cool; (4) release; (5) measure the strain recovery at zero load (γ_r) by counting the number of turns recovered, x, (6) determine fractional recovery f, where $f = x/5$.

A diagram showing the thermomechanical sequence of this experiment is shown in Fig. 1. The heating time is not of course instantaneous, but the set temperature is reached within 2–3 s. The relative humidity before, during and after the experiment was 40%.

In the previous study on PET [23], the heating rate was faster because the twisted monofilament was immersed in a hot oil bath. A comparison of air heating and oil heating of the PA66 yarn showed no significant dependence on the heating medium, but greater scatter in the heating data occurred when oil was used. This is probably due to residual oil on the multi-filament yarn interfering with recovery, and air was therefore chosen as the heating medium in this study.

The use of a multi-filament yarn also means that the strain conditions are relatively ill-defined in the PA66 study. In a twisted monofilament, the deformation mode is pure torsion, but in a multi-filament yarn each filament is deformed in both torsion and bending, and the ratio of these deformation modes depends on the radial position of the filament in the yarn. We can therefore provide only an approximate value of the imposed strain by considering the yarn bundle as a single filament of equivalent diameter. In this case the shear strain in the current experiments would be about 0.01. Experiments on PET monofilament have shown that heat-setting behavior in pure torsion and in pure bending (which is a combination of extension and compression) is qualitatively the same, but that the latter mode provides somewhat higher setting efficiency at all temperatures [25].

2.4. Crystallinity from density

Fiber density ρ was determined using a density gradient column at 23 °C. The column liquids used were carbon tetrachloride (CCl_4) and *n*-heptane. After being lowered into the gradient column, the fiber specimens were allowed 16 h for equilibration. Each density value reported is the average of three determinations. The volume fraction crystallinity of the PA66 fibers was calculated from $\chi = (\rho - \rho_a)/(\rho_c - \rho_a)$, where the crystalline density ρ_c was taken as 1240 kg/m^3 [26] and the amorphous density ρ_a was taken as 1090 kg/m^3 [26].

3. Results and discussion

3.1. Thermosetting of PA66 fibers

The decay in fractional 'twist' recovery f with heat setting temperature T_s for the partially oriented PA66 fibers is shown in Fig. 2, where the heat setting time t_s at each heat-setting temperature is 120 s. For the as-received fibers, f decreases monotonically with increasing T_s, whereas fibers that were pretreated at 150 °C and 200 °C for 30 min show a distinct plateau followed by a higher temperature setting process. For the presetting temperature T_p of 150 °C, the high temperature process begins at about 120 °C and for $T_p = 200$ °C, it begins at about 175 °C.

As discussed in the Section 2, the deformation mode of the fibers is a combination of torsion and bending, and the data in Fig. 2 confirms the general trends observed by Hearle et al., obtained from drawn PA66 monofilaments deformed in pure torsion [24]. The general phenomena are also similar to those observed in previous torsion heat-setting studies of PET monofilament. However, it is noticeable that for unpreset fibers, the reduction in fractional recovery occurs over a significantly broader temperature range in PA66 than in PET.

Since the properties of polyamide fibers can be sensitive to moisture content, we checked the influence of relative humidity on

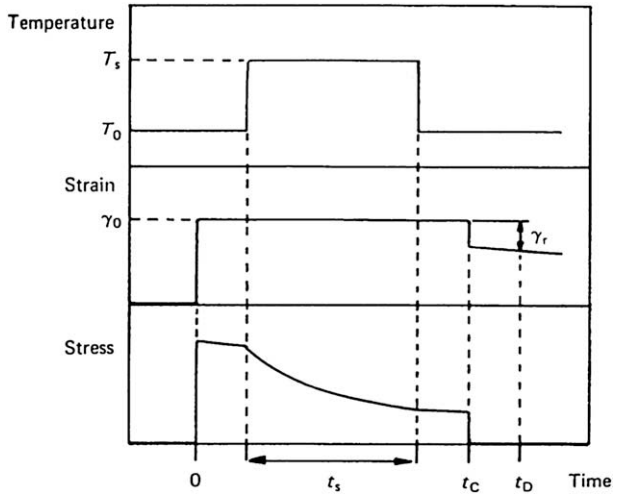

Fig. 1. Schematic diagram of the heat-setting sequence. (Adapted from Ref. [23]).

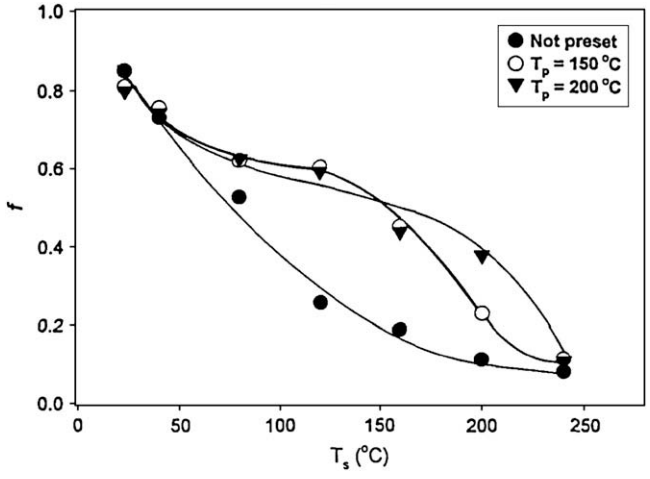

Fig. 2. Fractional recovery vs. heat-setting temperature for PA66 after various pre-setting conditions.

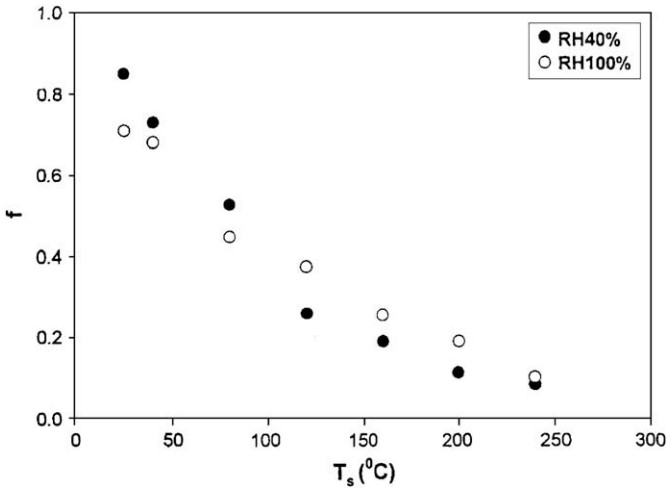

Fig. 3. Influence of relative humidity during sample-conditioning on fractional recovery of as-spun PA66 at various heat-setting temperatures.

the heat-setting behavior. Samples from the as-received PA66 fibers were immersed in water for seven days prior to heat setting. The yarns were then heat-set in torsion, and f was determined as a function of heat-setting temperature. It is evident from Fig. 3 that fibers conditioned at 100% relative humidity (RH) do not show significantly different heat-setting behavior from fibers conditioned at 40% RH. This may be because heat setting in air rapidly dries out the fibers, and the setting process takes place on relatively dry fibers irrespective of the initial moisture content.

Changes in crystallinity arising from heat-setting the PA66 fibers are shown in Fig. 4. The as-received fiber has a volume fraction crystallinity χ of about 0.3, and thermally-induced crystallization does not start to occur until T_s reaches a temperature of about 150 °C. However, increasing the crystallization time from 2 min to 30 min has a significant influence on the level of crystallinity achieved at a given temperature. For example, heating for 30 min at $T_p = 150$ °C causes χ to increase to 0.35 whereas the increase in χ is negligible at this temperature when the heating time is 2 min. Similarly, heating for 30 min at $T_p = 200$ °C results in a χ of about 0.47 compared with a value of 0.38 when the heating time is 2 min. This differs from PET fibers, where the rate of crystallization is much lower in this time interval [23]. A more complete picture of the development of crystallinity with time at various heat-setting temperatures is given in Fig. 5, from which it is apparent that

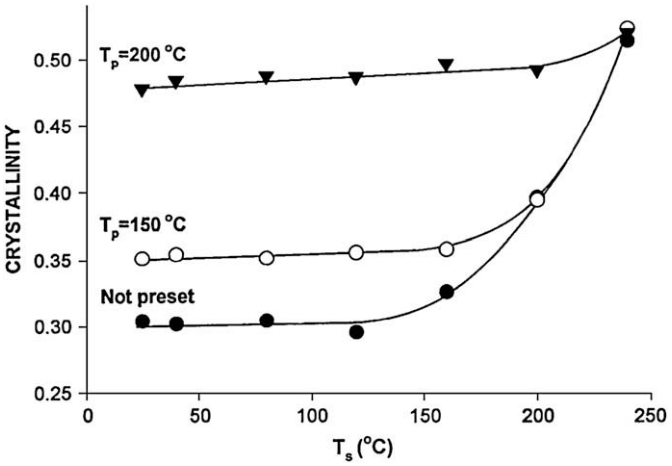

Fig. 4. Volume fraction crystallinity as a function of heat-setting temperature for PA66 fibers subjected to various presetting temperatures (where $t_p = 30$ min and $t_s = 2$ min).

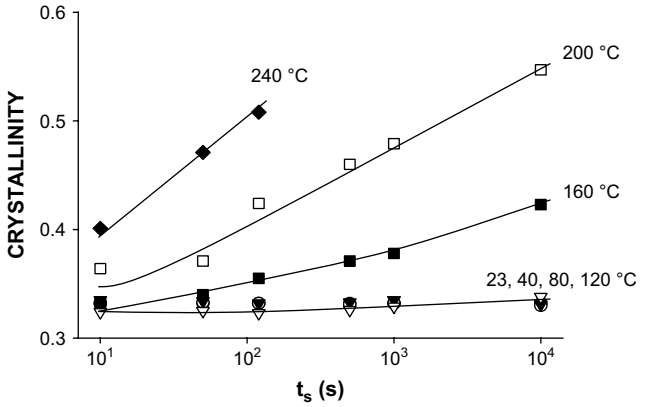

Fig. 5. Volume fraction crystallinity of PA66 fibers as a function of heat-setting time at various temperatures.

significant crystallization does not occur in these PA66 fibers until temperature significantly exceeds about 120 °C. Additional microstructure characterization of the PA66 fibers used in the present study has been reported elsewhere [27].

The focus of the present study is to explore the time dependence of thermosetting in PA66 fibers, since this is a crucial factor in providing predictive capability as well as in elucidating the molecular mechanisms underlying the process. It is evident from

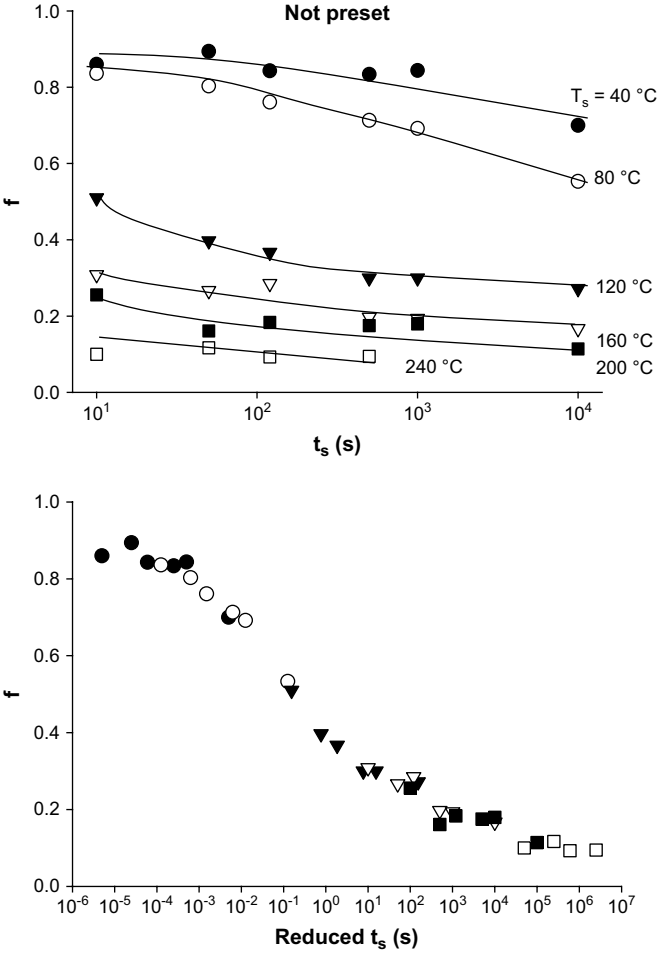

Fig. 6. Fractional recovery vs. heat-setting time at various heat-setting temperatures, for as-spun PA66 fibers (top), and the same data after shifting along the time axis to obtain a master curve with a reference temperature of 160 °C (bottom).

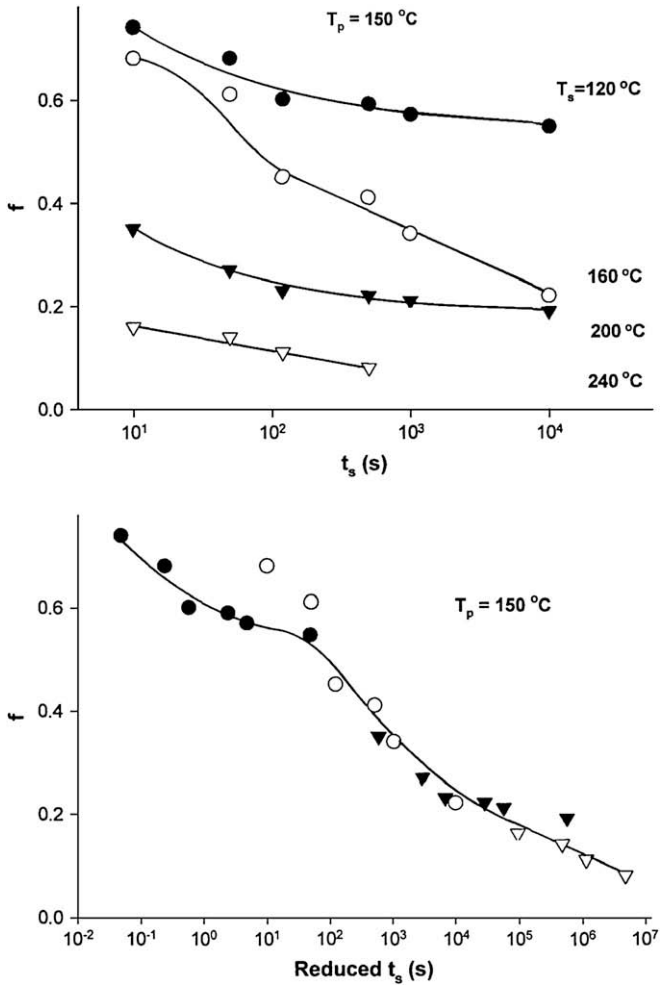

Fig. 7. Fractional recovery vs. heat-setting time at various heat-setting temperatures, for PA66 fibers preset at 150 °C (top); and the same data after shifting along the time axis to obtain a master curve with a reference temperature of 160 °C (bottom).

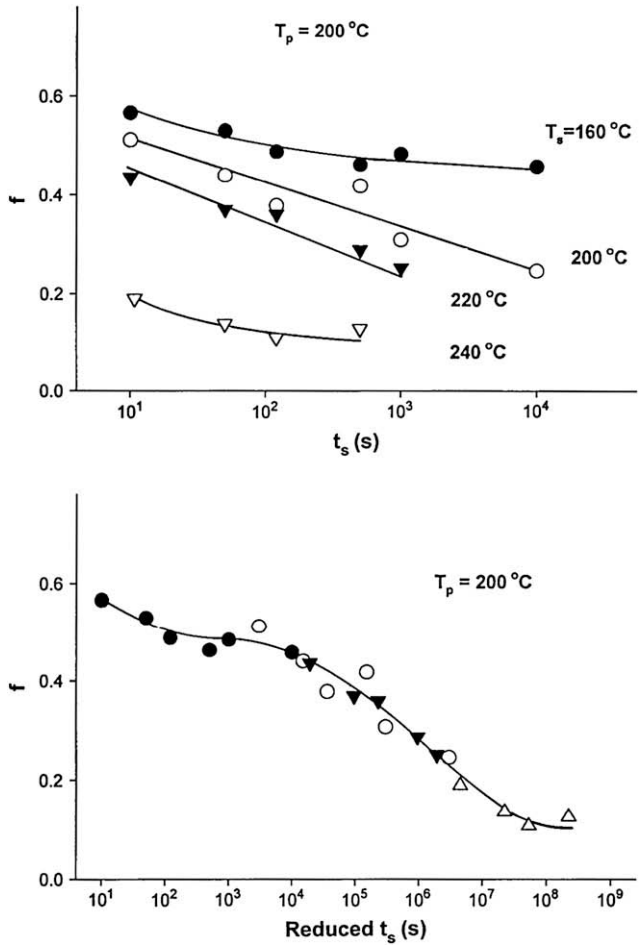

Fig. 8. Fractional recovery vs. heat-setting time at various heat-setting temperatures, for PA66 fibers preset at 200 °C (top); and the same data after shifting along the time axis to obtain a master curve with a reference temperature of 160 °C (bottom).

Fig. 6 (top), showing f vs. t_s for unpreset fibers, that f is indeed time-dependent and, as for poly(ethylene terephthalate) [23], the process responsible of thermosetting can be classified as an above-T_g relaxation, α'. Furthermore, by choosing an arbitrary reference temperature T_o of 160 °C, the curves in Fig. 6 (top) can be shifted to produce a master curve of f vs. reduced time (Fig. 6 (bottom)), demonstrating satisfactory time–temperature equivalence. In the reduced-time range from 10^{-3} s to 10^{8} s, the shape of the curve of f vs. t_s is very similar to the 'not preset' curve of f vs. T_s ($t_s = 120$ s) in the temperature range $T_s = 25$–240 °C (Fig. 2). The leveling off of f in the reduced-time curves at $t_s < 10^{-3}$ s would presumably become apparent on the f vs. T_s plot at temperatures below 25 °C.

For the presetting temperature of 150 °C ($t_p = 30$ min), the time dependence of f is shown in Fig. 7 (top). The master curve of f vs. reduced-time is reasonably satisfactory, with the exception of the data at 10 s and 50 s for $T_s = 160$ °C (Fig. 7 (bottom)). These inconsistent data points may arise from effects of the crystal–crystal Brill transition [28–31], which is known to occur in the region of 160 °C. For $T_p = 200$ °C ($t_p = 30$ min), shifting the f vs. t_s curves in Fig. 8 (top) produces the master curve of Fig. 8 (bottom).

The master curves for all three presetting conditions are plotted on the same graph in Fig. 9, and the clear resemblance of these curves to the curves of f vs. T_s in Fig. 2 provides strong support for the applicability of time–temperature equivalence. It appears, therefore, that the stress-relaxation behavior that permits permanent setting of partially crystalline PA66 is similar to that found in wholly amorphous polymers, except that crystallinity seems to impede the molecular motions responsible for stress decay, and

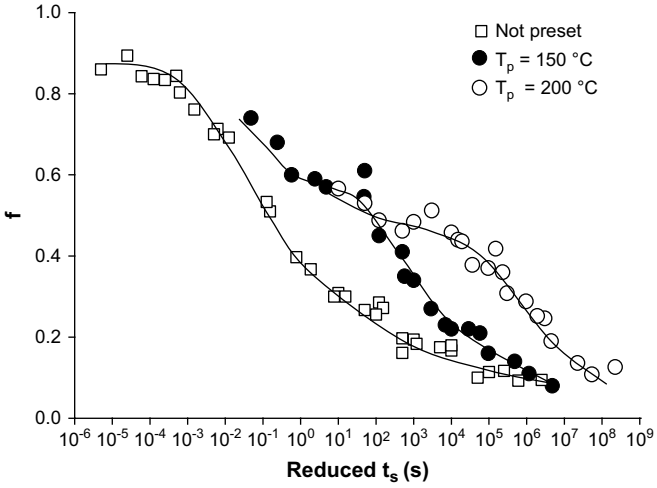

Fig. 9. Master curves of fractional recovery vs. reduced time for as-spun and preset PA66 fibers. The reference temperature is 160 °C.

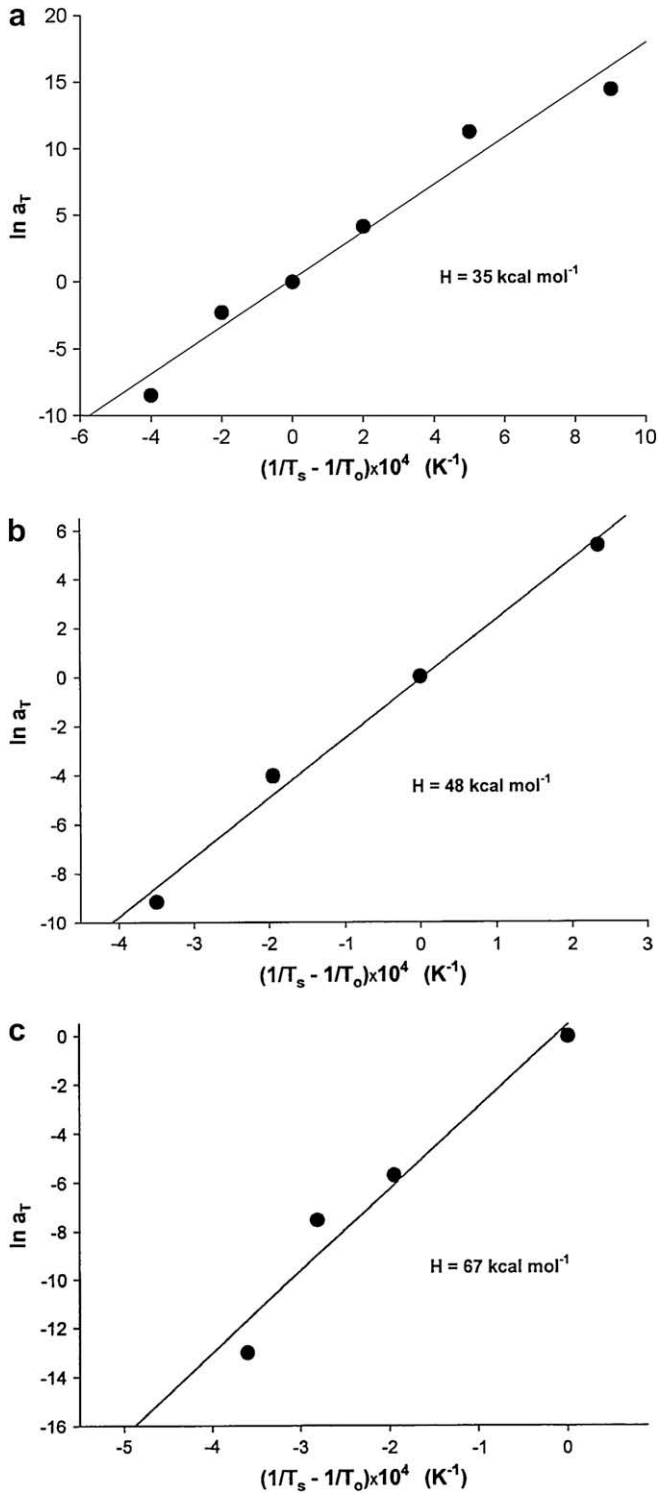

Fig. 10. Arrhenius plots for PA66 fibers (a) not preset, (b) preset at 150 °C, (c) preset at 200 °C.

increases the relaxation time in a similar way to an increase in molecular weight. It should be added, however, that other molecular rearrangements occurring during presetting could also have a significant, or strong, influence on constraining molecular motion during the heat setting process. For example, although the presetting treatment would be expected to relax stressed entanglements, this would be accompanied by thermally-induced

Table 1
Coefficients in Eqs. (2 and 3) for PA66 fibers.

Coefficient	$T_p = 150$ °C	$T_p = 200$ °C
a	6.1708513e-1	8.02825785e-1
b	−3.3853714e-3	−1.6125822e-1
c	8.3977873e-4	3.235385e-2
d	−2.746992e-3	−3.0618721e-3
e	3.9267848e-4	1.3179496e-4
f	−1.9666532e-5	−2.7763087e-6
g	3.2153371e-7	2.8980633e-8

formation of new entanglements in the unstressed state, and possibly to a higher entanglement density. The new distribution of entanglements, formed under the conditions of thermal mobility and time associated with a given presetting condition, would be expected to constrain relaxation in a subsequent thermosetting process.

It is important to notice that no vertical shifting of the data is required to achieve time–temperature superposition. This differs from the experience of Nagamatsu, Takemura and coworkers [32,33] who found that stress relaxation data in crystalline polyethylene can only be superimposed by introducing a vertical shift, which they consider to account for the effects of thermal crystallization occurring during the relaxation. Although crystallization is

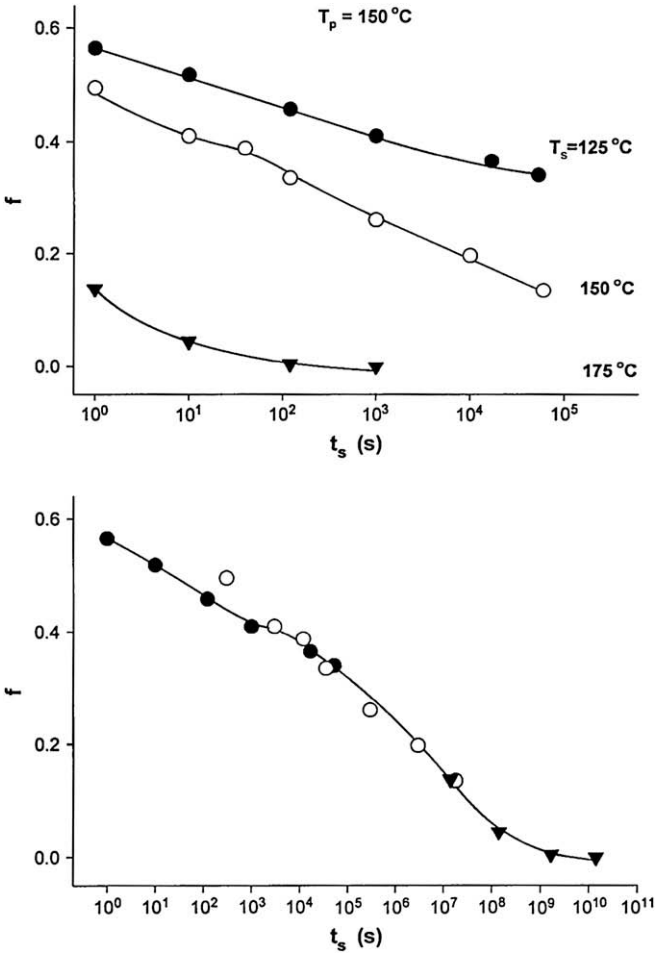

Fig. 11. Fractional recovery vs. heat-setting time at various heat-setting temperatures for PET monofilament preset at 150 °C (top); and the same data after shifting along the time axis to obtain a master curve with a reference temperature of 125 °C (bottom). The f/t_s data is from Buckley and Salem [23].

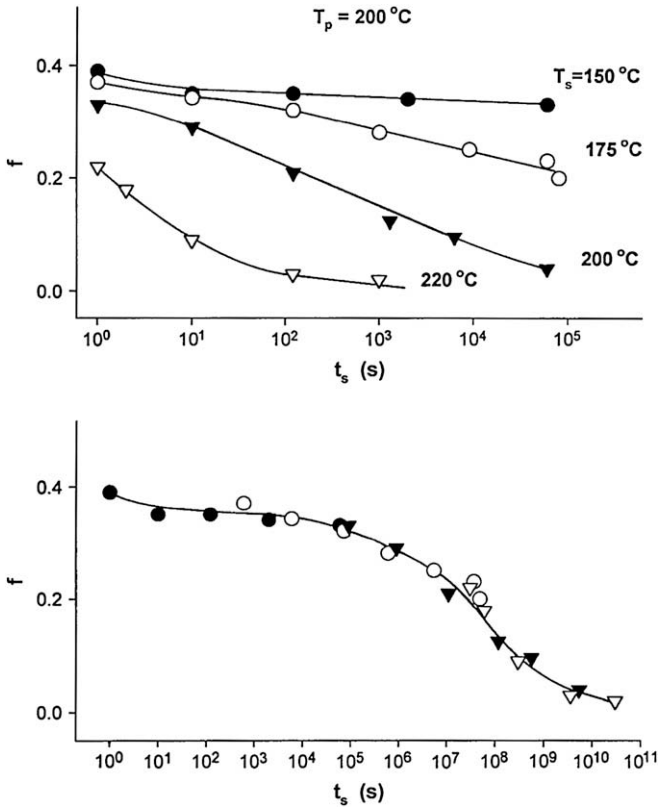

Fig. 12. Fractional recovery vs. heat-setting time at various heat-setting temperatures for PET monofilament preset at 200 °C (top); and the same data after shifting along the time axis to obtain a master curve with a reference temperature of 150 °C (bottom). The f/t_s data is from Buckley and Salem [23].

taking place during the heat setting of PA66, it appears to cause no obstacle to superposing the data by shifting only horizontally.

In view of the observed time–temperature superposition, it is of interest to determine nature of the time–temperature shift factor a_T and, if possible, the activation energy of the thermosetting process. An Arrhenius-type relationship has been found applicable to viscous flow processes in polymers above the glass transition temperature, in which

$$a_T = \exp\left[\frac{H}{R}\left(\frac{1}{T_s}-\frac{1}{T_o}\right)\right] \quad (1)$$

where R is the molar gas constant and H is the activation energy of the process.

Given that they are semi-log plots, the fit of the PA66 data to the Arrhenius equation (Fig. 10) can only be considered approximate in the case of the unpreset fibers and the fibers preset at 200 °C, whereas the fibers preset at 150 °C show better agreement. At any rate, the fits are sufficient to yield an approximate activation energy for viscous flow, which is in the range 35–67 kcal/mol, and they also permit approximate prediction of fractional recovery (thermosetting efficiency) at any time–temperature combination. For example, we have found that good empirical fits to the master curves at $T_p = 150$ °C and $T_p = 200$ °C can be described by:

$$f = a + b\ln t_s + c(\ln t_s)^2 + d(\ln t_s)^3 + e(\ln t_s)^4 + f(\ln t_s)^5 + g(\ln t_s)^6 \quad (2)$$

where the coefficients depend on T_p and are given in Table 1. By obtaining a_T for a particular setting temperature from Eq. (1), f can then be predicted at any setting time from:

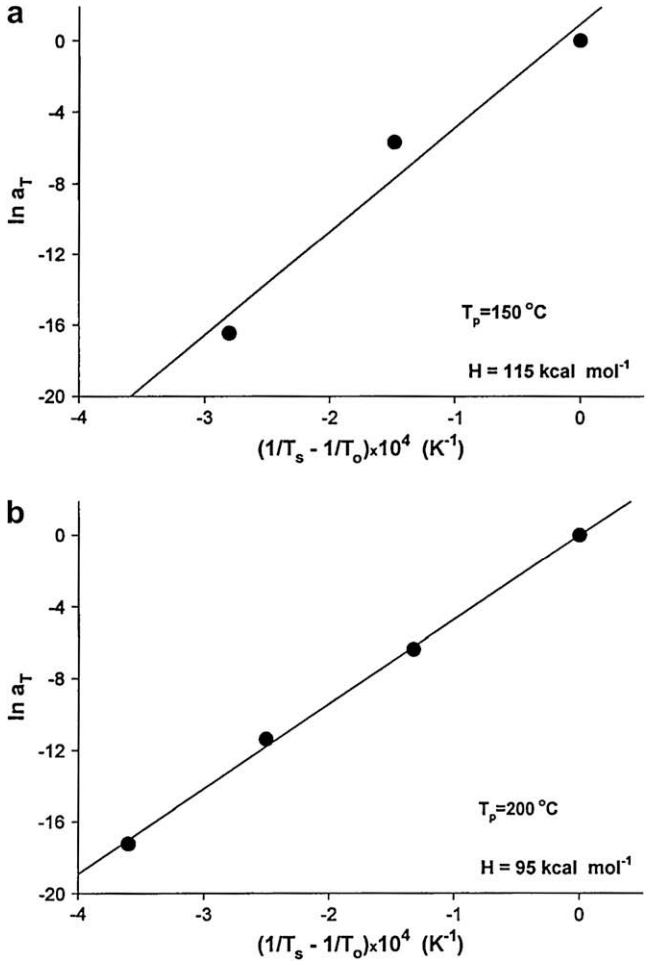

Fig. 13. Arrhenius plots for PET monofilament preset at (a) 150 °C and (b) 200 °C.

$$f = a + b\ln(t_s/a_T) + c\left[\ln(t_s/a_T)^2\right] + d\left[\ln(t_s/a_T)^3\right] + e\left[\ln(t_s/a_T)^4\right] + f\left[\ln(t_s/a_T)^5\right] + g\left[\ln(t_s/a_T)^6\right] \quad (3)$$

This formula can be of considerable practical value in assessing heat-setting behavior at shorter times than are readily accessible by experiment, but which are typical of time scales in industrial thermosetting operations. As an example, when $T_p = 150$ °C, f would be predicted to have a value of about 0.6 after heat setting at 200 °C for 0.1 s, compared with a value of about 0.35 after heat-setting for 10 s at 200 °C.

It should be noted that the temperature dependence of a_T could not be satisfactorily fitted to the Williams–Landel–Ferry equation.

3.2. Further analysis of PET thermosetting

The earlier studies by Buckley and Salem [23] on heat-setting poly(ethylene terephthalate) monofilament showed that f is strongly time-dependent and the plots of f vs. t_s at $T_p = 150$ °C and $T_p = 200$ °C were quite similar to those obtained in the present work for PA66 fibers. It is therefore of interest to attempt to shift the PET data obtained in Ref. [23], and to construct master curves that can be compared with the PA66 results.

As can be seen in Figs. 11 and 12, good master curves are obtained at both presetting temperatures, and Fig. 13 demonstrates the applicability of the Arrhenius equation. In this case, the better fit happens to be at the presetting temperature of 200 °C.

Table 2
Coefficients in Eqs. (2) and (3) for PET fibers.

Coefficient	$T_p = 150\ ^\circ C$	$T_p = 200\ ^\circ C$
a	5.6667787e-1	3.891945e-1
b	−4.0451986e-2	−3.4886158e-2
c	1.01036006e-2	1.11566854e-2
d	−1.6792361e-3	−1.7349894e-3
e	1.1622756e-4	1.28776e-4
f	−3.7314909e-6	−4.8619239e-6
g	4.6042724e-8	7.2111199e-8

Interestingly, the activation energy of about 100 kcal/mol is significantly higher than the values obtained for PA66, indicating that the relaxation rate in PET has a stronger temperature dependence.

The data at both $T_p = 150\ ^\circ C$ and at $T_p = 200\ ^\circ C$ can be well-fitted to Eq. (2) and the coefficients for these two presetting temperatures are given in Table 2, permitting prediction of fractional recovery at any combination of temperature and time from Eq. (3).

4. Conclusions

Thermosetting of PA66 and PET, in the oriented, semicrystalline state, is dominated by a high temperature relaxation process exhibiting time–temperature equivalence. Structural changes induced during thermal pretreatments constrain molecular motion in subsequent thermosetting, which delays onset of the flow regime and increases the time constant of relaxation at a given temperature.

Time–temperature superposition produces master curves for both PA66 and PET, and the shift factor can be approximately fitted to an equation of the Arrhenius-type. This permits prediction of heat-setting behavior at any combination of temperature and time, including shorter times than are accessible by experiment.

Although the thermosetting behavior of PA66 and PET fibers are phenomenologically similar, the activation energy of viscous flow associated with thermosetting in PA66 is in the range 35–65 kcal/mol compared with about 100 kcal/mol in PET.

Acknowledgments

This research was conducted at TRI/Princeton as part of a program sponsored by BASF, DSM, DuPont, Honeywell and Milliken. We are grateful to Dennis Briant of TRI/Princeton for his careful experimental work. Aspects of this work were presented at the Polymer Fibers 2002 International Conference, Manchester U.K.

References

[1] Schultz JM. In: Salem DR, editor. Structure formation in polymeric fibers. Munich: Hanser Publishers; 2001 [chapter 12].
[2] Oriani LAG, Simal AL. J Appl Polym Sci 1992;46:1973.
[3] Murthy NS, Minor H, Latif RAJ. Macromol Sci Phys B 1987;27:427.
[4] Murthy NS, Bray RG, Correale ST, Moore RAF. Polymer 1995;36:3863.
[5] Correale ST, Murthy NS. J Appl Polym Sci 2006;101:447.
[6] Salem DR, Moore RAF, Weigmann HD. J Polym Sci B 1987;25:567.
[7] Garcia D, Starkweather Jr HW. J Polym Sci Phys 1985;23:537.
[8] Coleman MM, Skrovanek DJ, Painter PC. Makromol Symp 1986;5:21.
[9] Simal AL, Martin AR. J Appl Polym Sci 1998;68:453.
[10] Vasanthan N, Ruetsch SB, Salem DR. J Polym Sci Polym Phys 2002;40:1940.
[11] Esposto LD, Koenig. J Polym Sci Polym Phys 1976;14:1731.
[12] Brody H. J Macromol Sci Phys 1983;B22(3):407.
[13] Pezkin PN, Schultz JM, Lin JS. J Polym Sci Polym Phys 1986;24:2591.
[14] Ward IM, Wilding MA. Polymer 1977;18:327.
[15] Lee KG, Schultz JM. Polymer 1993;34:4455.
[16] Busing WR. Macromolecules 1990;23:4608.
[17] Fu Y, Annis B, Boller A, Jin Y, Wunderlich B. J Polym Sci Polym Phys 1994;32:2289.
[18] Salem DR. In: Salem DR, editor. Structure formation in polymeric fibers. Munich: Hanser Publishers; 2001. p. 164–7.
[19] Castiff E, Tobolsky AV. J Colloid Sci 1955;10:375.
[20] Castiff E, Tobolsky AV. J Polym Sci 1956;19:111.
[21] Hearle JWS. In: Hearle JWS, Miles LWC, editors. The setting of fibers and fabrics. Watford: Merrow Publishing Co.; 1971 [chapters 1 and 5].
[22] Castiff E, Offenbach J, Tobolsky AV. J Colloid Sci 1956;11:48.
[23] Buckley CP, Salem DR. Polymer 1987;28:69.
[24] Hearle JWS, Wilding MA, Auyeung C, Ihmayed R. J Text Inst 1990;81:214.
[25] Buckley CP, Salem DR. J Appl Polym Sci 1990;41:1707.
[26] Nicols JB. J Appl Phys 1954;25:840.
[27] Vasanthan N, Salem DR. J Polym Sci B Phys 2000;38:516.
[28] Brill RJ. J Prakt Chem 1942;161:49.
[29] Brill RJ. Makromol Chem 1956;18/19:2940.
[30] Ramesh C, Keller A, Eltink SJEA. Polymer 1994;35:2483.
[31] Vasanthan N, Murthy NS, Bray R. Macromolecules 1998;31:8433.
[32] Nagamatsu K, Takemura T, Yoshimoto T, Takemoto T. J Polym Sci 1958;33:515.
[33] Takemura T. J Polym Sci 1959;38:471.